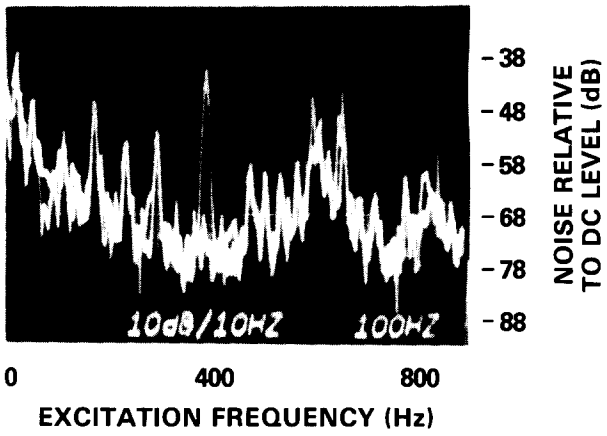

FIG. 3. Interferometer noise level, showing signal at 400 Hz due to 99 ppm NO_2 in nitrogen with 30-mW excitation at 514.5 nm.

operation at other than the optimal phase point and possible finesse degradation during the course of the experiment.

The noise floor at 400 Hz shown in Fig. 3 corresponds to a minimum detectable absorption (1-Hz detection bandwidth) of $1.3\times10^{-7}\,\mathrm{cm}^{-1}$ W (or 7 ppb NO_2 with 3-W excitation). Actual sensitivity was limited by a residual signal of -55.7 dB present even when the cell was continuously flushed with pure N_2. This limitation is attributed to synchronous heating of the optics and the adjacent air layers by the excitation beam, and could be overcome by coupling the excitation beams into the cavity transversely to the probe.

In order to estimate ultimate sensitivity limitations of the technique, we note that the noise floor ($\Delta f = 1$ Hz) of -83 dBV observed at 400 Hz is due to mechanical noise, $\langle \Delta L \rangle / L$, to which the cavity is as sensitive as to signal. Careful design of a stable etalon, deliberate choice of operating frequency at an acoustic null, and electronic subtraction of source amplitude noise should allow operation limited by shot noise, for our source, at -132 dBV. Density fluctuations in the sample will not limit sensitivity for samples at atmospheric pressure even of dimensions on the order of the He-Ne beam waist.

Shot noise limited detection with a cavity finesse of 50 corresponds to a phase sensitivity of 9×10^{-9} rad/($\sqrt{\text{Hz}}$). Considering the extreme stability required, this might be achievable only in sealed environments or condensed phase samples. A more reasonable phase sensitivity of 10^{-7} rad/($\sqrt{\text{Hz}}$) in our system with $L = 1$ cm corresponds to an absorption sensitivity of $1.9\times10^{-10}\,\mathrm{cm}^{-1}$ W.

We have demonstrated a simple interferometric technique for performing photothermal spectroscopy of transparent media with extreme sensitivity and spatial resolution.

[1] C. C. Davis, Appl. Phys. Lett. **36**, 515 (1980).
[2] J. P. Gordon, R. C. C. Leite, R. S. Moore, S. P. S. Porto, and J. R. Whinnery, J. Appl. Phys. **36**, 3 (1965).
[3] J. C. Murphy and L. C. Aamodt, J. Appl. Phys. **51**, 4580 (1980).
[4] A. J. Campillo, H-B. Lin, C. J. Dodge, and C. C. Davis, Opt. Lett. **5**, 424 (1980).
[5] C. C. Davis and S. J. Petuchowski, Appl. Opt. **20**, 2539 (1981).
[6] A. J. Campillo and H-B. Lin, SPIE Proc. **286**, 24 (1981).
[7] M. L. Swicord and C. C. Davis, Radio Sci. (in press).
[8] *Optoacoustic Spectroscopy and Detection*, edited by Y. H. Pao (Academic, New York, 1977).
[9] R. W. Terhune and J. E. Anderson, Opt. Lett. **1**, 70 (1977).

Imaging antenna array at 119 μm

Dean P. Neikirk, Peter P. Tong, and David B. Rutledge
Division of Engineering and Applied Science, California Institute of Technology, Pasadena, California 91125

Hyeon Park and Peter E. Young
Department of Electrical Sciences and Engineering, University of California, Los Angeles, California 90024

(Received 16 April 1982; accepted for publication 7 June 1982)

A focal-plane imaging antenna array has been demonstrated at 119 μm. The array is a line of evaporated silver bow-tie antennas with bismuth microbolometer detectors on a silicon substrate. Radiation is coupled into the array by a lens placed on the back of the substrate. The bolometers are thermally isolated from the silicon substrate with a half-micron layer of polyimide. The array performance is demonstrated by coherent imaging of a series of holes at half the diffraction-limited cut-off frequency.

PACS numbers: 42.80.Qy, 84.40.Jh, 07.62. + s, 85.40. − e

The use of a single detector and mechanically scanned optics is a well established technique in millimeter and submillimeter wave imaging.[1-3] However, in applications such as plasma diagnostics this approach is not adequate; the required integration time may be too long or the events too fast. A focal-plane array in monolithic integrated circuit form is an attractive solution in these cases. For both optical and infrared wavelengths focal-plane arrays of charge-coupled devices have been developed,[4,5] but the lack of suitable photoconductors in the far infrared ($\lambda \geqslant 100\,\mu$m) makes this technology difficult to apply there. An antenna array is appropriate at these longer wavelengths, and has been demon-

0003-6951/82/040329-03$01.00

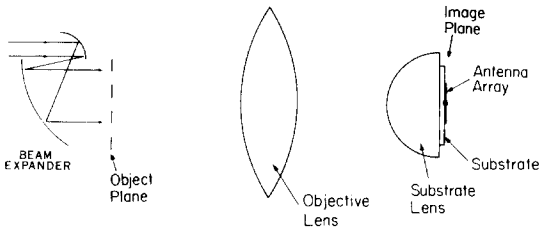

FIG. 1. Optical system used for imaging array.

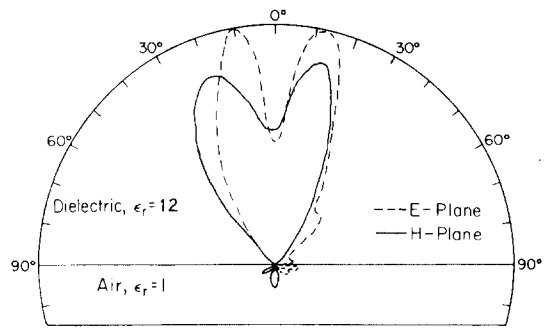

FIG. 3. Feed patterns of a single element in the bow-tie array.

strated at 1.2 mm.[6] Of primary interest in plasma diagnostics are wavelengths in the 100–1000-μm range, and this letter reports the successful demonstration of a 119-μm imaging system.

The basic optical system is shown in Fig. 1. Antennas on ungrounded substrates are most sensitive to radiation from the substrate side, and to take advantage of this, the radiation is coupled through the back of the substrate by a lens of the same dielectric constant.[7] At 100 μm absorption loss is high in most materials; at 2 dB/cm,[8] silicon is one of the lowest loss materials available. For this reason, both the substrate and the lens are high-resistivity silicon. The bow-tie antenna design[7] is shown in Fig. 2. The particular dimensions are chosen to give adequate sampling, impedance, and feed patterns. The antenna impedance is determined by the bow angle,[7] and is 80 Ω for a bow angle of 60°. Figure 3 shows the feed patterns, measured on microwave models with materials of dielectric constant 12 to match that of silicon.

Figure 4 is a photomicrograph of the actual 119-μm array. The substrate is 50-Ω cm silicon with 170 nm of thermally grown oxide to provide low-frequency isolation. The antennas are evaporated silver 100 nm thick and the detectors are bismuth microbolometers[9,10] 200 nm thick. All patterns are made with conventional contact photolithography and lift off. The dc resistances of the bolometers lay in the range of 50–60 Ω. Since the substrate has a large thermal conductivity it is necessary to thermally isolate the microbolometers from the silicon. This is done by spinning on a 500-nm-thick layer of DuPont Pyrallin 2555 polyimide between the bolometers and the substrate. The responsivity with the polyimide is 100 times higher than without the polyimide, and is comparable to the responsivity of bolometers on fused quartz.

The far-infrared measurements were made using a CO_2-pumped methanol laser.[11] The TPX plano-convex objective lens had a focal length of 65 mm. The silicon lens had a 3.88-mm radius of curvature and the lens-substrate combination had a total thickness of 5.0 mm. The entrance pupil of the system was limited by the size of the substrate lens, and was approximately 30 mm in diameter. This pupil size is used in the calculation of the succeeding diffraction limits. When focused at infinity, rotating the system 0.24° moved the focal spot from one antenna to the next. This corresponds to 0.96° per 100 μm in the image plane, agreeing well with the geometrical optics calculation of 0.94° per 100 μm. The useful image plane was 500 μm (20 antennas), limited by the size of the substrate lens. This gives an angular field of view of 5°. The system E-plane and H-plane patterns are shown in Fig. 5. These are measured by rotating the optical system and measuring the signal at a single antenna. The patterns are comparable in size to the theoretical diffraction-limited Airy pattern.

When used in imaging, the spatial cut-off frequency of the optical system is important in evaluating its performance. For this wavelength and entrance pupil the incoherent diffraction-limited cut-off frequency in the focal plane is 46 mm^{-1}. Our antenna spacing of 25 μm corresponds to a sampling frequency of 40 mm^{-1}; the effective cut-off frequency is one-half this sampling frequency. For diffraction-limited incoherent imaging, the antenna period causes undersampling of the image by about one-half.

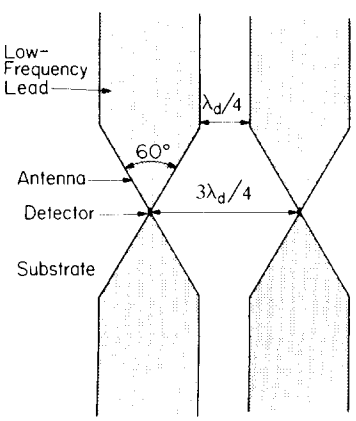

FIG. 2. Bow-tie antenna array designed for use on $\epsilon_r = 12$ substrate.

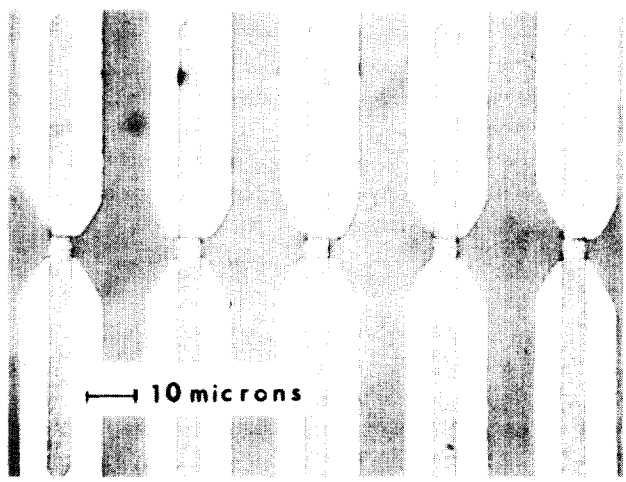

FIG. 4. Photomicrograph of a portion of the antenna array.

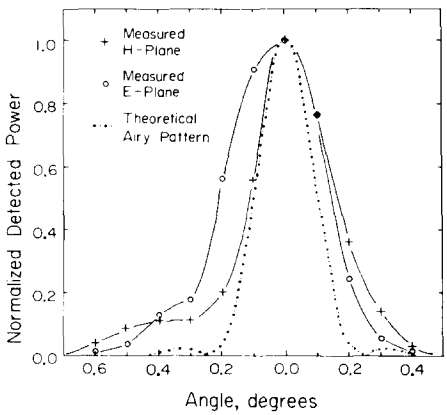

FIG. 5. System patterns at a single antenna.

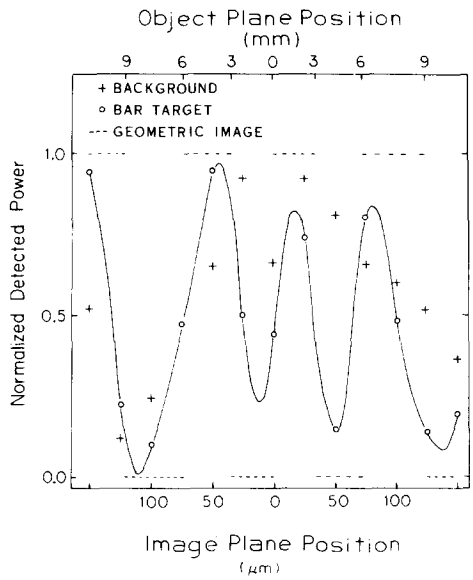

FIG. 6. Image of a 6-mm period bar target. The solid line is the sinc-function interpolation between the sampled data points. The relationship between object and image positions, measured from the optical axis, was determined by tracing rays parallel to the axis in the object plane.

In coherent imaging the diffraction-limited cut-off frequency is one half the incoherent cutoff; in this situation the image is not undersampled by the array. For our entrance pupil, and an object distance of 50 cm, the coherent cut-off frequency in the object plane is 0.3 mm^{-1}, a period of 3.3 mm. In our experiments, a copper plate with a series of 3-mm holes on 6-mm centers served as a resolution target. The fundamental frequency of the target is 0.17 mm^{-1}, approximately half the cut-off frequency. In order to uniformly illuminate the target, the gaussian output beam of the laser was passed through a beam expander (two cylindrical mirrors with focal length ratio 4:1). The target was placed 50 cm from the optical system, and viewed in transmission. The off-axis response of the imaging system is limited by spherical aberration of the plano-convex objective lens; exact ray tracing indicates a maximum useful off-axis distance of 10 mm in the object plane. This caused a roll off in signal from off-axis antennas when no object was present. Figure 6 shows this background roll off and the image of the target normalized to this envelope. The image is closed to the geometrical image found by ray tracing. Some difficulty has been encountered when imaging targets at these spatial frequencies, but this seems to be caused by the relatively small entrance pupil and off-axis response of the system; both should improve with the use of a longer focal length objective lens.

The microbolometer responsivity (without far-infrared system losses) was measured at 150 MHz.[10] The responsivity was 5 V/W with a 3-dB frequency response of 200 kHz. In order to determine the far-infrared system responsivity the total laser output power was measured with a model 3620 Scientech thermopile power meter. The optical system was then focused to yield the largest possible signal from a single antenna. The far-infrared response was a factor of 60 lower than the response at 150 MHz. This indicates that the optical system losses were 18 dB. These losses can be accounted for. The TPX used in the objective lens has a measured absorption loss of 4 dB/cm. The path length for this lens was about 2 cm, so 8 dB is lost here. The calculated loss of the silicon lens is 3 dB (2 dB reflection, 1 dB absorption). The remaining 7 dB probably results from a combination of factors: power absorbed by other antennas, optical system aberrations, the central dip in the feed pattern in Fig. 3, and irregularities in the laser output beam. The main source of loss is the objective lens and this would be reduced if it can be replaced by reflecting optics.

In conclusion, we have demonstrated a monolithic imaging antenna array at a wavelength of 119 μm, imaging a series of holes at half the coherent cut-off frequency. The key new feature is the thermal isolation of the bismuth microbolometer, enabling the use of low-loss silicon as a substrate material. The present limitations appear to be due to the objective lens used. With improvements in the optics, such as the use of reflecting components, improvements in the system efficiency and resolution should be possible.

We appreciate the support of the Jet Propulsion Laboratory and the Department of Energy under contract DeAM03-765F-00010 Task IIA. We would like to thank Professor S. E. Schwarz at U.C. Berkeley for helping us with the mask making, Professor N. C. Luhmann, Jr. and Dr. W. A. Peebles at UCLA for the loan of evaporators and facilities, and Professor D. Psaltis at Caltech for his insights on coherent imaging.

[1] J. P. Hollinger, J. E. Kenney, and B. E. Troy, Jr., IEEE Trans. Microwave Theory Tech. **MTT-24**, 786 (1977).
[2] D. T. Hodges, F. B. Foote, E. E. Reber, and R. L. Schellenbaum, Conference Digest, 4th Int. Conf. on Infrared and Millimeter Waves and Their Applications, IEEE Cat. No. 79 CH 1384-7 MTT, 1979, p. 51.
[3] J. Waldman, H. R. Fetterman, P. E. Duffy, T. G. Bryant, and P. E. Tannenwald, 4th Int. Conf. on Infrared and Millimeter Waves and Their Applications, IEEE Cat. No. 79 CH 1384-7 MTT, 1979, p. 49.
[4] J. T. Longo, D. T. Cheung, A. M. Andrews, C. C. Wang, and J. M. Tracy, IEEE Trans. Electron Devices **ED-25**, 213 (1978).
[5] D. F. Barbe, Proc. IEEE **63**, 38 (1975).
[6] D. P. Neikirk, D. B. Rutledge, M. S. Muha, H. Park, and C.-X. Yu, Appl. Phys. Lett. **40**, 203 (1982).
[7] D. B. Rutledge and M. S. Muha, IEEE Trans. Antennas Propag. **AP-30**, July (1982).
[8] C. M. Randall and R. D. Rawcliffe, Appl. Opt. **6**, 1889 (1967).
[9] T. L. Hwang, S. E. Schwarz, and D. B. Rutledge, Appl. Phys. Lett. **34**, 773 (1979).
[10] D. P. Neikirk and D. B. Rutledge, Appl. Phys. Lett. (to be published).
[11] D. T. Hodges, F. B. Foote, and R. D. Reel, Appl. Phys. Lett. **29**, 662 (1976).